International Conference on Space Optics—ICSO 2014

La Caleta, Tenerife, Canary Islands

7–10 October 2014

Edited by Zoran Sodnik, Bruno Cugny, and Nikos Karafolas

An experiment to test in-field pointing for Elisa

Christina Brugger

Bernhard Broll

Ewan Fitzsimons

Ulrich Johann

et al.

esa icso proceedings cnes

International Conference on Space Optics — ICSO 2014, edited by Zoran Sodnik, Nikos Karafolas, Bruno Cugny, Proc. of SPIE Vol. 10563, 105634D · © 2014 ESA and CNES
CCC code: 0277-786X/17/$18 · doi: 10.1117/12.2304152

AN EXPERIMENT TO TEST IN-FIELD POINTING FOR ELISA

Christina Brugger[1], Bernhard Broll[1], Ewan Fitzsimons[1], Ulrich Johann[1], Wouter Jonke[2], Stefano Lucarelli[1], Susanne Nikolov[1], Martijn Voert[2], Dennis Weise[1] and Gert Witvoet[2]
[1] *Airbus DS GmbH, 88039 Friedrichshafen, Germany*
[2] *TNO Opto Mechatronics, 2600 AD Delft, Netherlands*

I. INTRODUCTION

The evolved Laser Interferometer Space Antenna (eLISA) Mission is being developed to detect and characterise gravitational waves by measuring pathlength changes between free flying inertial test masses over a baseline of order 1 Gm [1]. Here the observed astrophysical events and objects lie in a frequency range between 30 µHz and 1 Hz (the LISA measurement band, LMB).
Within the eLISA Mission, orbital dynamics cause the shape of the constellation to change over a period of one year. As a result, the angle between the interferometer arms varies by a few degrees on an annual timescale and must be actively compensated for. Most studies looking at eLISA type missions typically feature the Telescope Pointing concept - articulating the two telescopes with a mechanism and adjusting the entire payload to compensate. One possible alternative concept which has been studied in the LISA Mission Formulation study carried out by Astrium Satellites Germany (now Airbus DS) is to utilise In-Field Pointing (IFP) [2]. With IFP, a small mechanism would tilt a mirror positioned at an intermediate pupil of a wide field telescope, thus providing the required pointing corrections. IFP possesses inherent advantages over Telescope Pointing in that it removes the need to articulate large parts of the payload, does not require a backlink fibre to connect adjacent arms, can result in smaller payload sizes and enables payload architectures with only one test mass per spacecraft. Demanding requirements are, however, placed on the optical properties of the telescope and the stability of the mechanism.

II. MEASUREMENT PRINCIPLE AND KEY OBJECTIVES

To demonstrate the feasibility of IFP, we are developing an experiment – co-funded with DLR (national astronautics and space research centre of Germany) – to perform an end-to-end experimental validation of the IFP concept. The experiment will feature a wide-field off-axis telescope with a prototype In-Field Pointing Mechanism (developed by TNO) located at an intermediate pupil. A heterodyne interferometer will be used to measure the performance aspects specific to In-Field Pointing.
In addition to measuring the passive stability the dependence of the optical pathlength through both the mechanism and the telescope surfaces on the pointing angle can be investigated. Thus piston generated directly at the mechanism and due to systematic beam steering over the mirror topography within the telescope can be studied [3]. Moreover the coupling of pointing jitter to local topography gradients on mirror surfaces and the impact of misalignments, i.e. geometrical lever arms coupling to pointing jitter, can be analysed.
The overall contribution to the displacement noise in the LMB should be less than 3 pm/$\sqrt{\text{Hz}} \times u_{pl}(f)$ with the basic noise shape $u_{pl}(f)$ for pathlength related quantities relaxing as $1/f^2$ at frequencies below 3 mHz. Additionally, the derivative pathlength change over the field of view should be less than 2 pm/nrad.

III. TELESCOPE DESIGN FOR IN-FIELD POINTING

The optical design is a fully representative wide-field off-axis telescope because without obscuration stray light into the receive path is minimised. In comparison to former studies [4] the aperture has been downscaled to 15 cm which is still a representative size to show the feasibility of In-Field Pointing. With a seasonal variation in the angle of the interferometer arms of about 1.2° (peak to peak, 1Gm arm length), the minimum required field of view is ± 0.6°. The instantaneous field of view (Inst. FoV) or the maximum acquisition range to be accommodated is 200 µrad. The optical telescope design consists of two stages with a total magnification of 25. The first stage includes three mirrors with a magnification of 5 producing an accessible intermediate pupil with a diameter of 30 mm. The In-Field Pointing Mechanism, which compensates for the breathing is located here. Two folding mirrors (plane mirrors) are also used to keep the setup compact.

With the telescope covering a full field of view of ± 1° the In-Field Pointing Mechanism has been designed with a ± 2.5° tilt range (i.e. ± 5° tilt of the beam).
The second stage of the optical telescope design contains a pupil relay system with a magnification of 5 producing a pupil of 6 mm in diameter. Finally a pupil relay system with a magnification of 1 on the interferometer breadboard allows pupil imaging onto a photo receiver where it is mixed with the reference beam. A summary of the optical telescope design and its significance in the context of eLISA is shown in Fig. 1.

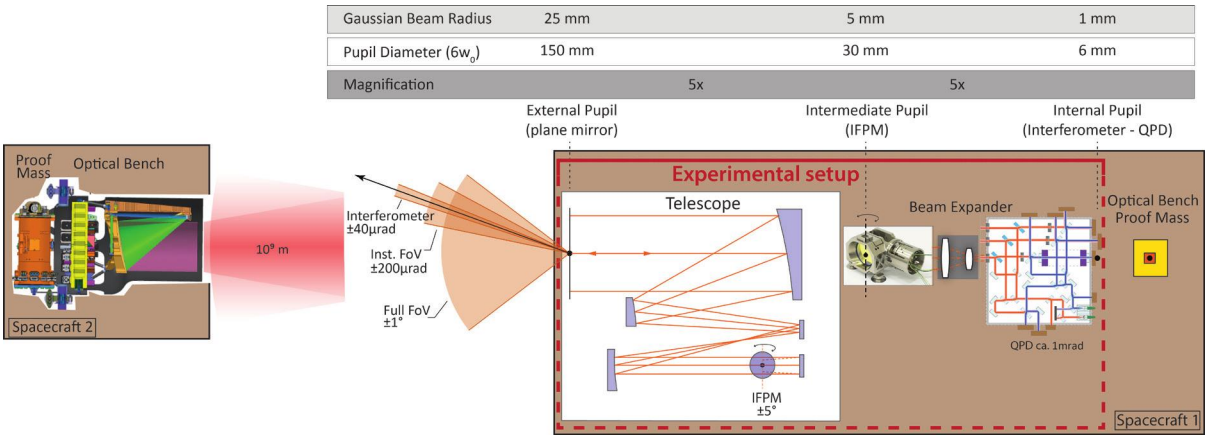

Fig. 1: Summary of the optical design for In-Field Pointing including a telescope design for an external aperture of 15 cm, the In-Field Pointing Mechanism, a Beam Expander (5x) and the heterodyne interferometer for signal measurement. The sketch illustrates the function and significance of IFP for eLISA.

When designing the optical telescope some constraints have to be considered in order to meet the requirements outlined in section II. One of the most important aspects is that the design has to guarantee the required optical performance over the entire field of view meaning that neither the pupil stability nor the wavefront error (WFE) quality should differ much from former baselines [4]. For the telescope imaging in its ideal design configuration a wavefront error of λ/30 rms at the design wavelength of 1064 nm and a value for piston coupling in the range of 0.3 pm/nrad can be achieved. Note that both values refer to a single path through the telescope beginning from the external pupil to the photo receiver at the internal pupil.
Moreover it is important to provide an accessible intermediate pupil at the position of the In-Field Pointing Mechanism, and still have a robust and stabile setup with respect to alignment errors or manufacturing tolerances of the optical components. Tolerance analysis for the telescope (1st and 2nd stage) and the relay system on the interferometer board showed that an overall WFE of λ/25 rms can be achieved. For this analysis the whole optical path (from the interferometer to the external pupil and back to the photo receiver), tolerances for manufacturing, alignment and during operational stability have been taken into account.

IV. IN-FIELD POINTING MECHANISM

After having developed a conceptual design, the In-Field Pointing Mechanism (IFPM) was manufactured and assembled by TNO (Netherlands Organisation for Applied Scientific Research) in the Netherlands [4]. It is a pointing device in which a stable incident beam is deflected from a flat mirror with a diameter of 50 mm that can be tilted to accomplish the beam steering over the required beam tilt range of ± 5° (i.e. ± 2.5° mirror tilt). The mechanism is based on a monolithic TiAl 5 structure with integrated elastic Haberland hinges designed for the required mirror rotation range of at least ± 2.5°. With the size of about 70x70x130 mm³ it weights roughly 1 kg. A gimbal architecture, in which the axis of rotation ideally coincides with the mirror surface, minimises sensitivity of the optical pathlength to pointing variations. To minimise mirror surface distortion the actuation force, based on a pizeo stepper mechanism, is parallel to the mirror surface. Herein a ceramic beam guided by the piezo steppers is used to achieve a high resolution in combination with a large range. This actuator concept works with a clamp-step motion in which a regulation of the piezo driving voltage can accurately define the actuator position between the steps.
With a required absolute pointing knowledge of ± 10 µrad it has to provide a pointing rate for the beam of 25 nrad/s in science mode while not exceeding a beam pointing jitter at the IFPM of 10 nrad/√Hz within the LMB, corresponding to 2 nrad/√Hz at the external pupil of the telescope [4].

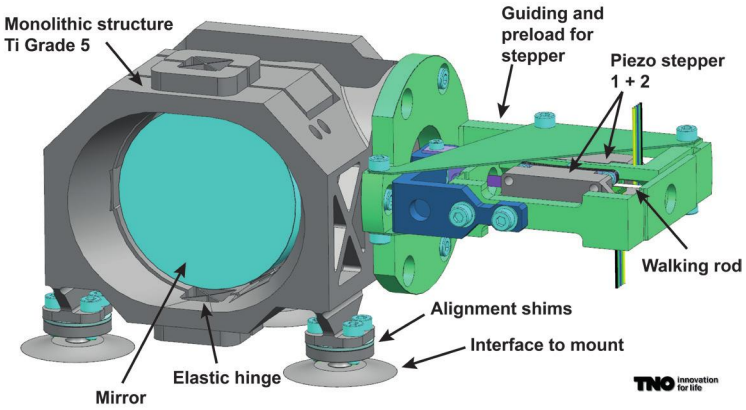

Fig. 2: CAD model of the In-Field Pointing Mechanism (designed and manufactured by TNO) based on a monolithic TiAl 5 structure including an elastic hinge and two piezo steppers for actuating the mirror.

V. EXPERIMENTAL SETUP

In Fig. 3 a CAD model illustrates the experimental setup showing the main elements and the way they are mounted to the optical bench. The mounts for all optical elements are entirely in Zerodur to guarantee a good thermal stability. On the optical bench with a size of about 1.1x0.8 m² the setup includes the following main elements:

- A heterodyne interferometer for signal measurement (internal pupil on a photo receiver)
- A wide-field off-axis telescope consisting of 1st and 2nd stage (total magnification: 25)
- The In-Field Pointing Mechanism at an intermediate pupil of the telescope
- An external pupil (plane mirror)

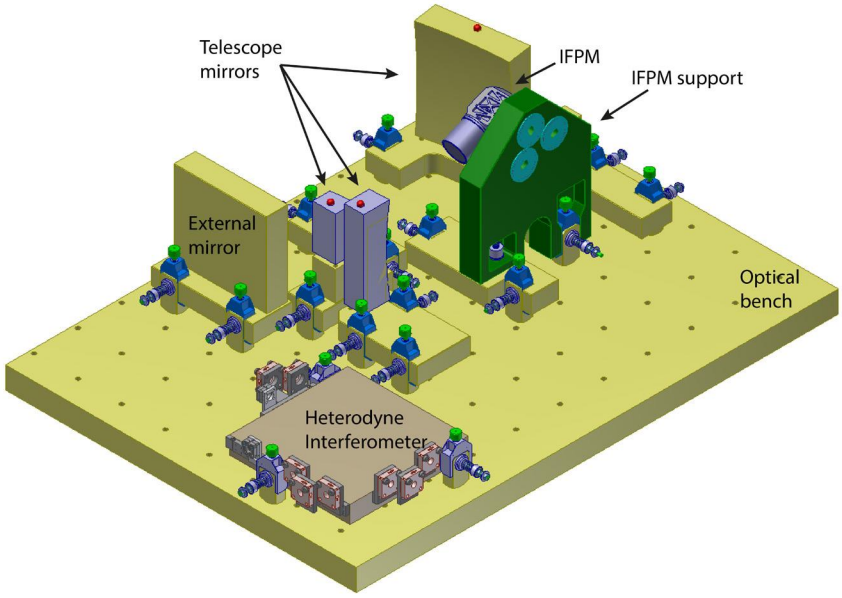

Fig. 3: CAD model of the experimental setup with the main elements on the optical bench: Heterodyne interferometer, IFPM including its Zerodur support (green block), telescope mirrors and external pupil (plane mirror).

Measurements of pathlength changes will be accomplished with a heterodyne interferometer similar in optical design to that used for the optical bench in the LISA Technology Package [5]. It is constructed on a Zerodur breadboard with a size of 270x275 mm² and utilises fibre injectors provided by the University of Glasgow to ensure a highly constant beam pointing [6] [7] (Fig. 4). It operates with a heterodyne frequency of 10 kHz and detects the interfered signal of measurement and reference beam with Quadrant Photodiodes (QPD) enabling tilt measurements by Differential Wavefront Sensing (DWS) [8] [9]. Fig. 3 shows the optical layout of the heterodyne interferometer for signal measurement with a design sensitivity of < 1 pm/√Hz including the relay system for pupil imaging on the photo receiver.

Beside the use of Zerodur for critical elements to reduce thermal expansion, it is also important to have a compact design and a minimum of transmissive elements in the optical path not only for the interferometer but also for the telescope. In this way changes in the optical pathlength caused by a change in the refractive index due to temperature fluctuations (dn/dT and CTE) are avoided.

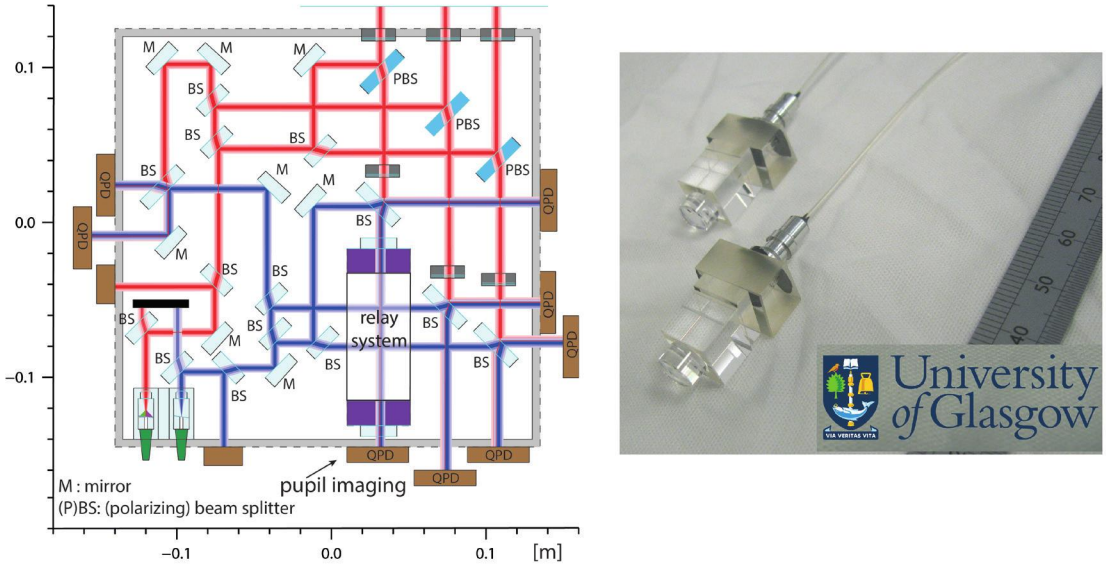

Fig. 4: OptoCAD [10] model of the heterodyne interferometer for signal measurement. Measurement and reference beam are provided by two monolithic fibre injectors (manufactured by the University of Glasgow) shown on the right that ensure a highly constant beam pointing.

The optomechanical support for all optics and especially for the telescope mirrors is based on a 3-point kinematic mounting concept (Fig. 5 on the right). Herein each mirror is attached to 3 spheres fitting into its lower surface. The mount is realized by the spheres lying in a conical hole, in a V-groove and on a flat surface, enabling a removable and repeatable repositioning of the mounted mirror.
The main parts of the setup (meaning the plane mirror at the external pupil, the telescope mirrors, the IFPM support and the interferometer head) can be aligned in all degrees of freedom with a 3-feet mounting concept [11] [12] [13] (Fig. 5 on the left) which was specifically designed for guaranteeing minimal thermal expansion.

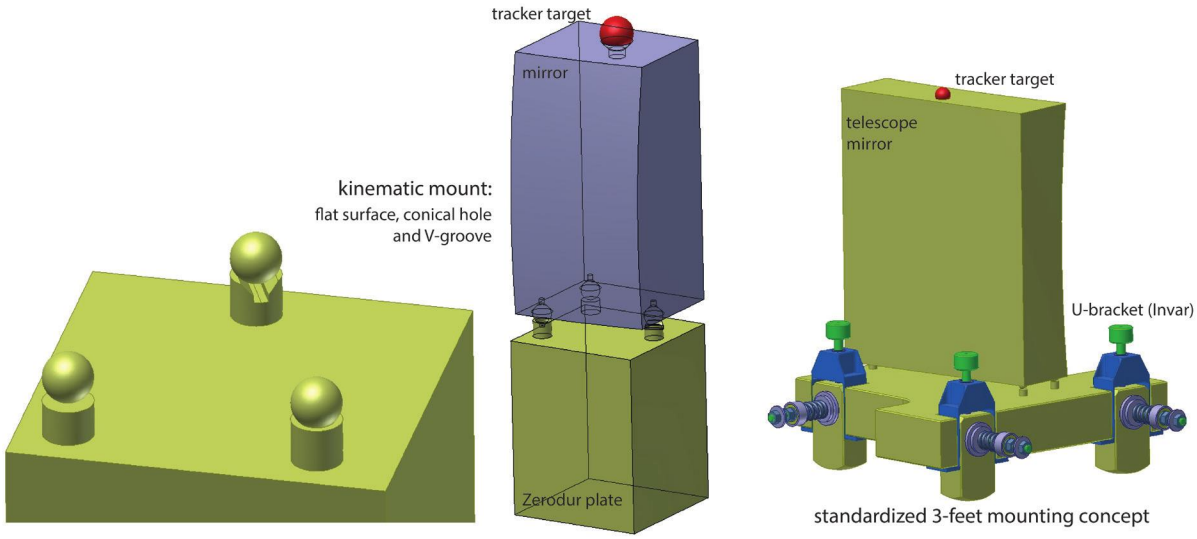

Fig. 5: 3-point kinematic mounting concept for the mounting of the telescope mirrors onto a Zerodur plate (on the left). In the middle the interface between mirror (blue) and Zerodur plate standing on the optical bench is shown. One of the telescope mirrors with the 3-feet mounting concept for the alignment on the optical bench can be seen on the right. In order to use the laser tracker for alignment the mirrors are equipped with a spherical tracker target (red) on top.

To ensure the required performance, the mirrors of the telescope must be aligned to an accuracy of 5 µm and 10-20 µrad. The alignment will be accomplished utilising standard optical instruments (laser tracker, theodolite, Shack-Hartman wavefront sensor). Therefore each mirror is equipped with a spherical tracker target on top (red balls in Fig. 5) as well as polished back surface and sides. The position of the target is calibrated such that the distance to the vertex of the mirror is known to an accuracy of 10 µm and the reference surfaces polished such that the angles between each surface and the optical axis are known to an accuracy of 20''.
For the in-plane translation and rotation around the axis micrometre screws are used. They will be placed around the relevant components and fixed with tape onto the bench. After a successful alignment these screws can be removed again.

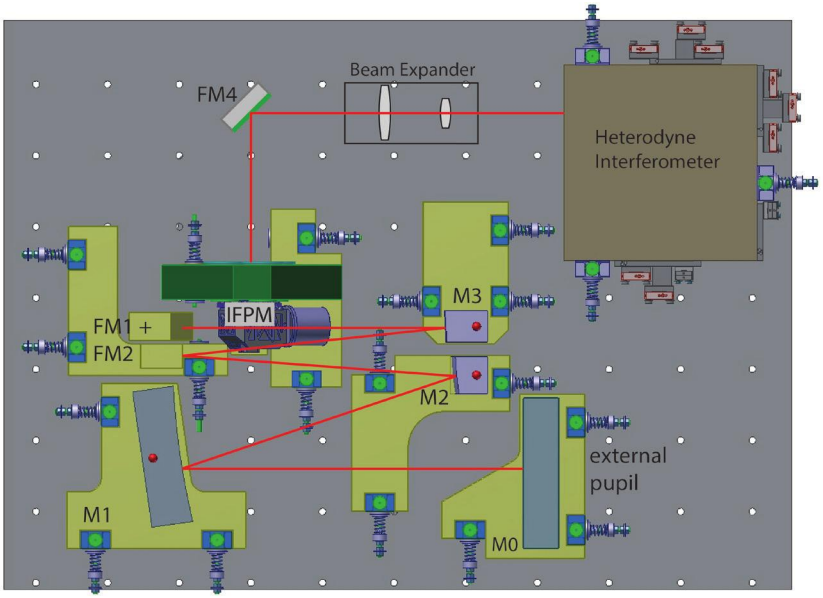

Fig. 6: CAD model of the experiment. It shows the interferometer board (Zerodur) without the optical components on top but with all photodiodes attached to its sides and the out and in coming beam (red line). All other main elements shown on the optical bench are the Beam Expander, the IFPM mounted to a Zerodur block (green), the telescope mirrors (M1, M2, and M3), the folding mirrors (FM1, FM2, and FM4) and the external pupil which is a plane mirror (M0). The missing folding mirror FM3 can't be seen from top as its position is underneath the mechanism.

The experiment will be constructed in a vacuum chamber with integrated thermal shielding consisting of Aluminium and multi-layer insulation. Around the vacuum tank another 15 cm thick styrodur layer will help to minimise temperature fluctuations intruding from the laboratory environment.

VI. TESTING

In the case of IFP the variation of the inter-arm angle is around ≈ 1.2° (peak to peak) at the external pupil. The example orbit shown in Fig. 7 gives a maximum required pointing rate of $v_{max} = 4$ nrad/s and a root mean square value of $v_{rms} = 1.7$ nrad/s (Fig. 8). In the experiment the external pupil is a fixed plane mirror. So a rotation of the IFPM mirror changes the angle of reflection at the external pupil as well as the incident angle at the photo receiver. As the field of view of the QPD at the internal pupil is limited, a given pointing rate leads to a specific measurement frequency.

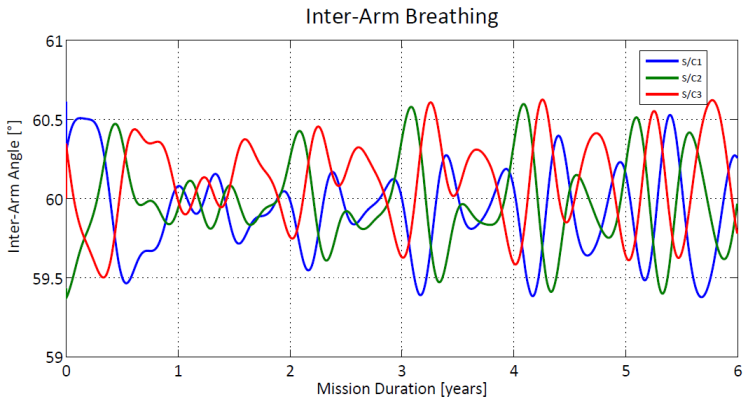

Fig. 7: Inter-arm breathing in degrees for an arm length of 1 Gm between the spacecraft.

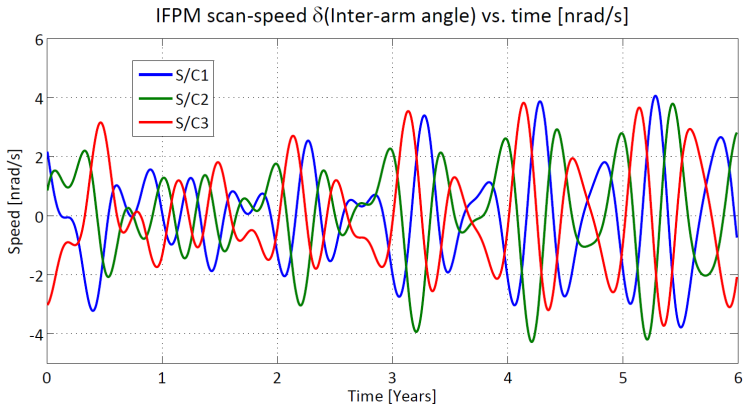

Fig. 8: Pointing rates in nrad/s calculated from the example orbit shown in Fig. 7 that have to be compensated. Maximum pointing rates are in the range of 4 nrad/s and the root mean square value is 1.7 nrad/s.

Making a rough estimation for a QPD with a maximum field of view of about 1 mrad and taking the maximum pointing range of 4 nrad/s, reasonable and useful data can only be taken for about 1×10^{4} s. This leads to measurement frequencies down to 1×10^{-4} Hz. The measurement with a plane mirror at the external pupil will be done by scanning with the IFPM over the field of view of the QPD for different static angular positions of the plane mirror at the external pupil (and the IFPM scan mirror respectively).
Beyond that it would be desirable to replace the plane external pupil. Therefore two options will be taken into account. First of all a corner cube consisting of two mirrors perpendicular to each other could be used. In this case an out coming beam (from the heterodyne interferometer) would be reflected back in the same direction and thus allowing a scan over the whole external field of view (± 1°) without being limited to the field of view of the QPD (± 40µrad at external pupil). In addition one would not have to change the position of the external pupil and avoid misalignment. However the option of a motorized plane mirror at the external pupil will be considered, too. Thus a simultaneous scan of the IFPM mirror and the motorized external mirror could cover the full field of view.

REFERENCES

[1] European Space Agency, "LISA, Unveiling a Hidden Universe," *Assessment Study Report,* 2011.
[2] D.Weise, P. Marenaci, P. Weimer, M. Berger, H. R. Schulte, P. Gath, U. Johann, "Opto-Mechanical Architecture of the LISA Instrument," *Proceedings of the 7th ICSO,* Barcelona, Spain, 2008.
[3] H. Kögel, D. Gerardi, J. Pijnenburg, M. Gohlke, T. Schuldt, U. Johann, C. Braxmaier, and D. Weise, "Interferometric characterisation and modelling of pathlength errors resulting from beamwalk across mirror surfaces in LISA," *Applied Optics*, Vol. 52, Issue 15, pp. 3516-3525, 2013.
[4] D. Weise, P. Marenaci, P. Weimer, H. R. Schulte, P. Gath, and U. Johann, „Alternative Opto-Mechanical Architectures for the LISA Instrument," *Journal of Physics: Conference Series,* Vol. 154 Issue 1, 2009.
[5] D. I. Robertson, et. al., "Construction and testing of the optical bench for LISA Pathfinder," *Class. Quantum Grav.*, Vol. 30, Issue 8, 2013.
[6] A. Taylor, et. al., *ASP Conference Series*, 998, 2012.
[7] Killow C., Fitzsimons E.D., Perreur-Lloyd M., Robertson D.I., Ward H., Bogenstahl J., "Quasi-monolithic fibre couplers suitable for spaceflight," unpublished.
[8] E. Morrison, B. J. Meers, D.I. Robertson, H. Ward, "Automatic Alignment of Optical Interferometers," *Applied Optics*, Vol. 33, Issue 22, pp. 5041-5049, 1994.
[9] E. Morrison, B. J. Meers, D. I. Robertson, H. Ward, "Experimental Demonstration of an Automatic Alignment System for Optical Interferometers," *Applied Optics*, Vol. 33, Issue 22, pp. 5037-5040, 1994.
[10] R. Schilling, "OptoCad – A Fortran 95 module for tracing Gaussian TEM_{00} beams through an optical set-up," www.rzg.mpg.de/~ros/Optocad
[11] Schuldt T., Gohlke M., Kögel H., Spannagel R, Peters A., Johann U., Weise D. and Braxmaier C., „Picometer Interferometry and its Application in Dilatometry and Surface Metrology," *Proceedings of the 10th ISMTII*, 2011.
[12] E. Stoppel, "Precision Dilatometry on low CTE samples," *Master Thesis*, February 2011.
[13] M. Gohlke, T. Schuldt, D. Weise, U. Johann, A. Peters, C. Braxmaier, "Development and Validation of Key Enabling Technologies for LISA Optical Metrology," *Proceedings of the 8th LISA Symposium*, Stanford, 2010.